DOI 10.5162/Ultrasonic2025/C1-a5

Real-Time Adaptive Ultrasonic Plane Wave Imaging towards Online Automated Curved Structure Inspection

Zhixuan Chang[1,2], Shiwei Wu[1], Keji Yang[1,2], and Haoran Jin[1,2]
[1] Zhejiang University, State Key Laboratory of Fluid Power and Mechatronic Systems, School of Mechanical Engineering, Hangzhou, China
[2] Zhejiang University, The Key Laboratory of Advanced Manufacturing Technology of Zhejiang Province, Hangzhou, China
chang_zhixuan@zju.edu.cn, jinhr@zju.edu.cn

Abstract: Phased array ultrasonic imaging is widely utilized in industrial non-destructive testing and evaluation (NDT&E). With advancements in robotics technology, phased array probes can be mounted on manipulators to autonomously inspect complex curved structures in water-immersed environments, enhancing both inspection capacity and efficiency. Conventional Delay-And-Sum (DAS) based imaging techniques require prior knowledge of the structure's surface geometry and the relative position of the probe. The acoustic path with the shortest time of flight is then determined based on Fermat's principle. However, the inspection Pulse Repetition Frequency (PRF) and the number of pixels are constrained due to the computational cost of the acoustic path searching and DAS operations. Although several optimization methods have been proposed to accelerate or bypass the searching process, inspection performance remains limited by DAS operations. Alternatively, recursive non-stationary phase shift migration based imaging method have been developed to eliminate DAS operations, but their efficiency remains unsatisfactory. In this paper, we propose an adaptive wavenumber domain plane wave imaging method that enables real-time online imaging with fine spatial resolution. Each imaging cycle contains a group of emission events. In the first imaging cycle, conventional wavenumber domain plane wave imaging is employed to reconstruct the surface geometry as an initialization step. From the second imaging cycle onward, the emission focal law is dynamically adjusted based on the reconstructed surface geometry from the latest previous cycle, enabling the generation of steered plane wavefronts beneath the curved couplant-specimen interface. Once the scattering echoes are captured, non-stationary phase shift migration techniques are applied to simultaneously reconstruct both the surface geometry and the scattering wavefield beneath the specimen surface. Finally, the wavenumber domain f-k migration method is utilized to reconstruct inspection images with high computational efficiency. Simulations were conducted to validate the proposed method. The real-time online imaging frame rate exceeds 45 fps, with about 200 thousands pixels in the ROI, demonstrating the potential of the proposed method for automated industrial online NDT&E.

Keywords: Ultrasonic non-destructive testing, Curved structure inspection, Ultrasonic imaging, Adaptive plane wave imaging, High-frame-rate imaging

Introduction

Curved structures are widely deployed in industrial applications, such as pipes, rails, pressure vessel, and so on. It's crucial to detect the internal flaws in such structures as early as possible to ensure the safety. Phased array ultrasonic testing technology is widely utilized due to its environment suitability. The Full Matrix Captured (FMC) based Total Focus Method (TFM) has been widely used for specimen inspection due to its high image quality and precision[1]. However, when inspecting curved structures, determining the focal delay for each pixel requires searching for the minimum acoustic time-of-flight path based on Fermat's principle, introducing heavy computation burden and limiting the imaging frame rate and image resolution [2]. Although sparse matrix operation and Graphic Process Unit (GPU) based methods are utilized to accelerate the computation, the imaging frame rate is still not satisfying especially when the image resolution is large [3]. Plane Wave Imaging (PWI) is an alternative approach to FMC which can reduce emission cycles to generate an inspection image without sacrifice on the image quality [4]. However, these methods requires the prior knowledge of the structure geometry, limiting the implementation of such methods in industrial applications.

DOI 10.5162/Ultrasonic2025/C1-a5

Several dynamic imaging methods has been established to overcome the dependence on the prior knowledge of the structure geometry [5], [6]. The basic idea is measuring the surface geometry online and then calculating focal delay. This further increases the time complexity of the reconstruction process. Another approach is set a group of virtual sources on the boundary of the structure with few emission cycles, and then calculate the focal delay inside the structure [7]. This method avoid the searching process brought by Fermat's principle, but still depends the calculation of focal delay in isotropic medium and DAS algorithm. There are also a kind of method use single emission cycle to generate low quality image at high frame rate, and then use learning based method to improve the image quality [8], but their generalization capacity still needs more verification.

Besides DAS based imaging approaches, wavenumber domain imaging methods are also widely utilized in ultrasonic imaging [9]. These methods convert the scattering wavefield to wavenumber domain with Fourier transform, and then reconstruct wavenumber domain image with a nonlinear mapping, which can realize ultrafast imaging frame rate [10], [11]. These methods have been adapted to curved structure imaging with non-stationary wavefield extrapolation theory [12]. This study presents an adaptive imaging method based on the wavenumber domain non-stationary plane wave imaging method. In each imaging cycle, the surface geometry of the structure is extracted from the reconstructed image, and emission delays are calculated for the next cycle. Simulation based on k-Wave is utilized to validate the proposed method. An real-time imaging frame rate of 45 fps is achieved, highlighting the potential of the proposed method.

Methods

Wavenumber domain cross-correlation imaging condition is utilized to measure the geometry of the wavefield, whose operations share significant overlap with NSPWI method [12].

Considering that the incident wave and received scattering wave are both one-way waves, hence the general analytical forms of incident waves P_i and scattering waves P_s are given by

$$\begin{aligned} P_s(k_x, z, \omega) &= K_2(k_x, \omega) e^{-\imath k_z z}, \\ P_i(k_x, z, \omega) &= K_1(k_x, \omega) e^{\imath k_z z}, \end{aligned} \tag{1}$$

where k_z is the wavenumber along z-axis, which can be calculated by dispersion relation

$$k_z = \operatorname{sgn}(\omega) \sqrt{(\omega/c)^2 - k_x^2}. \tag{2}$$

When $z = 0$, the incident wavefields and scattering wavefield is already known,

$$\begin{aligned} &P_s(k_x, z = 0, \omega) = \iint p_s(x, t) e^{-\imath(k_x x + \omega t)} dx dt, \\ &P_i(k_x, z = 0, \omega) \\ &\quad = \iint S(\omega) A(x) e^{-\imath(k_x x + \omega(t - t_j))} dx dt. \end{aligned} \tag{3}$$

where $S(\omega)$ is the response signal spectrum of an element, $A(x)$ is the apodization function of the array, t_j is the emission delay of the jth element. Hence,

$$\begin{aligned} P_s(k_x, z, \omega) &= P_s(k_x, z = 0, \omega) e^{\imath k_z z}, \\ P_i(k_x, z, \omega) &= P_i(k_x, z = 0, \omega) e^{-\imath k_z z}. \end{aligned} \tag{4}$$

According to the cross-correlation imaging condition, the inspection image in isotropic medium is given by[13]

$$I(x, z) = \iint P_s(k_x, z, \omega) P_i^*(k_x, z, \omega) e^{\imath k_x x} d\omega dx, \tag{5}$$

From the reconstructed image in couplant layer, the acoustic boundary can be extracted by finding pixels with the maximum intensity in each image column,

$$\hat{f}_1(x) = \max_z I(x, z). \tag{6}$$

where $z = f(x)$ is the acoustic boundary curve function. Then the plane wave beamforming algorithm stated in [4] is utilized to calculate the emission delays for next FMC frame. Since the emission delays calculation requires the normal of the acoustic boundary, a cubic smoothing spline $z = \hat{f}_2(x)$ is deployed to reconstruct the directly extracted acoustic boundary with a tolerance of 0.1 mm. The defects consist of a group of Side-Drilled-Holes (SDHs), as illlustrated in Fig. 1.

The imaging scene is illustrated as Fig. 1. Let $p_l(x, t)$ be the scattering wavefield with a steered angle of θ_l, the surface geometry is given as $\hat{f}_2(x)$ from the results of the last imaging cycle. The top and bottom boundaries of the nonstationary interval is the minimum and maximum values of $\hat{f}_2(x)$ respectively

$$h_0 = \min_x \hat{f}_2(x), \quad h_1 = \max_x \hat{f}_2(x). \tag{7}$$

In nonstationary interval, the sound speed is piecewise constant, (4) should be modified to

$$\begin{aligned} &P(k_x, z + \Delta z, \omega) \\ &\quad = \sum_i \left(\alpha_i(k_x, \omega) \mathcal{F}_x W_i\right) \mathcal{F}_{k_x}^{-1} P(k_x, z, \omega), \end{aligned} \tag{8}$$

DOI 10.5162/Ultrasonic2025/C1-a5

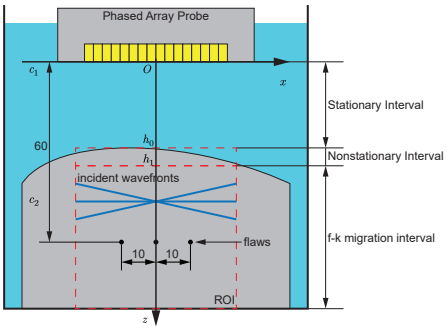

Fig. 1: Imaging scene illustration.

where $\alpha_i(k_x, \omega)$ is the wavefield extrapolation factor in the ith medium

$$\alpha_i(k_x, \omega) = \exp\left(\imath \Delta z \sqrt{(\omega/c_i)^2 - k_x^2}\right). \quad (9)$$

Subsequently, the image within the nonstationary interval can be reconstructed using (5) and (9), yielding $P(k_x, h_1, \omega)$ required by the next f-k migration imaging step. In fact, the scattering wavefield is determined by the scatterers distribution with steered incident wavefronts[12]

$$S_i(k_u(k_x, k_2), k_v(k_x, k_2)) = e^{\imath\omega\sigma_i}\sqrt{k^2 - k_x^2} P\left(k_x(k_u, k_v), z = h_2, k_2(k_u, k_v)\right), \quad (10)$$

where $\boldsymbol{k}_2$ is the wavenumber vector in the second layer medium, and k_u, k_v are given by

$$\begin{aligned} k_x(k_u, k_v) &= k_x - k_2 \sin\theta_i, \\ k_2(k_u, k_v) &= \frac{k_u^2 + k_v^2}{2k_u \sin\theta_i + 2k_z \cos\theta_i}. \end{aligned} \quad (11)$$

Finally, the reconstructed image in f-k migration interval is obtained by

$$I(u, v) = \left| \mathcal{F}^{-1}_{k_u, k_v} \sum_i S_i(k_u, k_v) \right|. \quad (12)$$

Results and Discussion

Simulation is designed to verify the proposed method. The deployed phased array probe has 64 elements with a pitch of 0.6 mm, a width of 0.5 mm. The center frequency of the probe is 5 MHz, and the sampling rate is set to 295 MHz to make sure the CFL of the simulation less than 0.3. In the imaging phase, a 4 subdivision of the sampling rate is used to make the sampling rate more similar to practical configurations. The sound speed of the specimen is set to $c_2 = 5900$ m/s, and that in other area is set to $c_1 = 1483$ m/s. The steered angle of the incident planar wavefronts is set to from -4° to 4° with a step of 1°.

The surface geometry extracted from the image is shown in Fig. 2 (a). The directly detected boundary and smoothed boundary are plotted in black and red lines, respectively. It is obvious that the smoothed boundary has a better precision for normal estimation. The emission delays calculated with the smoothed boundary is shown in Fig. 2 (b). Compared with the exact values obtained from the precise boundary measurements, the error is smaller than 102.4 ns.

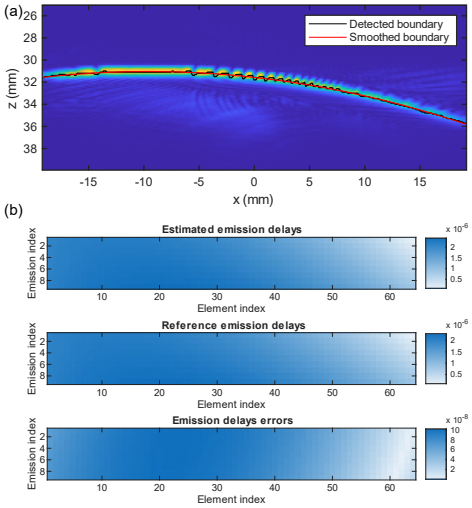

Fig. 2: (a) Extracted boundary and smoothed boundary. (b) Estimated emission delays and estimation error.

Reconstructed image using estimated emission delays are illustrated in Fig. 3 (a). It can be seen that the surface geometry and the SDHs are all identified, although the surface exhibits higher intensity compared to the SDHs due to energy attenuation during wave propagation across the acoustic boundary. The red rectangular area is the ROI which contains flaws. The reconstructed image in ROI is normalized and compressed with log function and plotted in Fig. 3 (b). The exact position of the flaws are plotted with red circles. The maximum intensity projection along depth direction is shown in Fig. 3 (c). The imaging algorithm was implemented using CUDA to accelerate the computation, and a final frame rate of 45 fps is achieved on a commercial computer with a CPU of Core U7 265K ((Intel Corporation, Santa Clara, CA, USA)) and a GPU of RTX 3070Ti (NVIDIA Corporation, Santa Clara, CA, USA).

Conclusion

In this work, we presented an adaptive real-time ultrasonic imaging for curved structure inspection with high frame rate and high image resolution. Wavenumber domain non-stationary wavefield extrapolation and

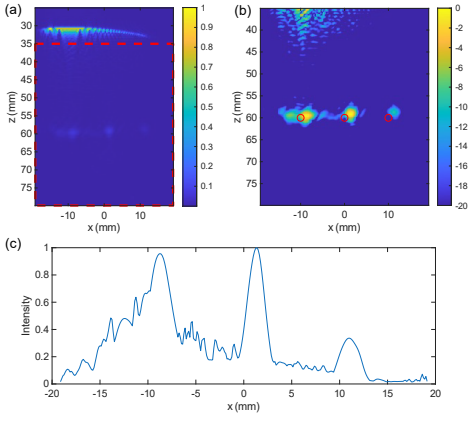

Fig. 3: (a) Reconstructed image. (b) The normalized ROI reconstructed image after log transformation. (c) The maximum intensity projection curve along depth direction.

cross-correlation algorithm were employed to measure the surface geometry during the continuous imaging process. After that the wavenumber domain f-k migration method was applied to reconstruct images with high efficiency. Simulation results showed that the proposed method can achieve high image quality and a frame rate of 45 fps, highlighting the potential of the proposed method for online automated curved structure inspection.

References

[1] C. Holmes, B. W. Drinkwater and P. D. Wilcox, 'Post-processing of the full matrix of ultrasonic transmit–receive array data for non-destructive evaluation,' *NDT & E International*, vol. 38, no. 8, pp. 701–711, 2005.

[2] L. Le Jeune, S. Robert and C. Prada, 'Plane wave imaging for ultrasonic inspection of irregular structures with high frame rates,' in *42ND ANNUAL REVIEW OF PROGRESS IN QUANTITATIVE NONDESTRUCTIVE EVALUATION: Incorporating the 6th European-American Workshop on Reliability of NDE*, Minneapolis, Minnesota, 2016, p. 020 010.

[3] G. Y. Hou et al., 'Sparse Matrix Beamforming and Image Reconstruction for 2-D HIFU Monitoring Using Harmonic Motion Imaging for Focused Ultrasound (HMIFU) With In Vitro Validation,' *IEEE Transactions on Medical Imaging*, vol. 33, no. 11, pp. 2107–2117, 2014.

[4] G. Cosarinsky, J. Fernandez-Cruza and J. Camacho, 'Plane Wave Imaging through Interfaces,' *Sensors*, vol. 21, no. 15, p. 4967, 2021.

[5] L. Le Jeune, S. Robert, P. Dumas, A. Membre and C. Prada, 'Adaptive ultrasonic imaging with the total focusing method for inspection of complex components immersed in water,' in *41ST ANNUAL REVIEW OF PROGRESS IN QUANTITATIVE NONDESTRUCTIVE EVALUATION: Volume 34*, Boise, Idaho, 2015, pp. 1037–1046.

[6] J. Wang, Z. Zhou, Y. Li, G. Yang and W. Zhou, 'A high efficiency adaptive ultrasonic array imaging method with sensitivity correction for curved structures,' *Measurement*, vol. 238, p. 115 322, 2024.

[7] J. F. Cruza and J. Camacho, 'Total Focusing Method With Virtual Sources in the Presence of Unknown Geometry Interfaces,' *IEEE Transactions on Ultrasonics, Ferroelectrics, and Frequency Control*, vol. 63, no. 10, pp. 1581–1592, 2016.

[8] F. Zhang, L. Luo, J. Li, J. Peng, Y. Zhang and X. Gao, 'Ultrasonic adaptive plane wave high-resolution imaging based on convolutional neural network,' *NDT & E International*, vol. 138, p. 102 891, 2023.

[9] M. H. Skjelvareid, T. Olofsson, Y. Birkelund and Y. Larsen, 'Synthetic aperture focusing of ultrasonic data from multilayered media using an omega-K algorithm,' *IEEE Transactions on Ultrasonics, Ferroelectrics and Frequency Control*, vol. 58, no. 5, pp. 1037–1048, 2011.

[10] J.-y. Lu, '2D and 3D High Frame Rate Imaging with Limited Diffraction Beams,' *IEEE Transactions on Ultrasonics, Ferroelectrics and Frequency Control*, vol. 44, no. 4, pp. 838–856, 1997.

[11] Jiqi Cheng and Jian-yu Lu, 'Extended high-frame rate imaging method with limited-diffraction beams,' *IEEE Transactions on Ultrasonics, Ferroelectrics and Frequency Control*, vol. 53, no. 5, pp. 880–899, 2006.

[12] Z. Chang et al., 'An efficient ultrasonic wavenumber-domain plane wave imaging method towards the inspection of curved structures,' *Ultrasonics*, vol. 143, p. 107 416, 2024.

[13] R. Ali, 'Fourier-based Synthetic-aperture Imaging for Arbitrary Transmissions by Cross-correlation of Transmitted and Received Wavefields,' *Ultrasonic Imaging*, vol. 43, no. 5, pp. 282–294, 2021.